

The Search for Higgs particles at high-energy colliders: Past, Present and Future

ABDELHAK DJOUADI

Laboratoire de Physique Mathématique et Théorique, UMR5825-CNRS,
Université de Montpellier II, F-34095 Montpellier Cedex 5, France.

Abstract

I briefly review the Higgs sector in the Standard Model and its minimal Supersymmetric extension, the MSSM. After summarizing the properties of the Higgs bosons and the present experimental constraints, I will discuss the prospects for discovering these particle at the upgraded Tevatron, the LHC and a high-energy e^+e^- linear collider. The possibility of studying the properties of the Higgs particles will be then summarized.

*Review talk given at the Workshop on High-Energy Physics Phenomenology,
WHEPP VII, Harish-Chandra Research Institute,
Allahabad, India, January 4-15, 2002*

1. Introduction

The search for Higgs bosons is one of the main missions of present and future high-energy colliders. The observation of this particle is of major importance for the present understanding of the interactions of the fundamental particles. Indeed, in order to accommodate the well-established electromagnetic and weak interaction phenomena, the existence of at least one isodoublet scalar field to generate fermion and weak gauge bosons masses is required. The Standard Model (SM) makes use of one isodoublet field: three Goldstone bosons among the four degrees of freedom are absorbed to build up the longitudinal components of the massive W^\pm, Z gauge bosons; one degree of freedom is left over corresponding to a physical scalar particle, the Higgs boson [1]. Despite of its numerous successes in explaining the present data, the SM will not be completely tested before this particle has been experimentally observed and its fundamental properties studied.

In the SM, the profile of the Higgs particle is uniquely determined once its mass M_H is fixed [2]. The decay width, the branching ratios and the production cross sections are given by the strength of the Yukawa couplings to fermions and gauge bosons, the scale of which is set by the masses of these particles. Unfortunately, the Higgs boson is a free parameter.

The only available information on M_H is the upper limit $M_H \geq 114.1$ GeV established at LEP2 [3]. [The collaborations have also reported a 2.1σ excess of events beyond the expected SM backgrounds consistent with a SM-like Higgs boson with a mass $M_H \sim 115$ GeV [3], as will be discussed later.] Furthermore, the accuracy of the electroweak data measured at LEP, SLC and the Tevatron provides sensitivity to M_H : the Higgs boson contributes logarithmically, $\propto \log(M_H/M_W)$, to the radiative corrections to the W/Z boson propagators. A recent analysis yields the value $M_H = 88_{-37}^{+60}$ GeV, corresponding to a 95% CL upper limit of $M_H \lesssim 206$ GeV [4] [there is still an error due to the hadronic contribution to the running of the fine structure constant α]; see the left panel in Fig. 1.

However, interesting theoretical constraints can be derived from assumptions on the energy range within which the Standard Model is valid before perturbation theory breaks down and new phenomena would emerge.

(i) If the Higgs mass were larger than ~ 1 TeV, the W and Z bosons would interact strongly with each other to ensure unitarity in their scattering at high energies. Imposing the unitarity requirement in the scattering of longitudinal W bosons at high-energy for instance leads to the tree-level bound $M_H \lesssim 870$ GeV [5]. Note also that radiative corrections to the Higgs boson couplings become non-perturbative for masses beyond $M_H \gtrsim 1$ TeV [6] and the Higgs resonance becomes too wide as will be discussed later.

(ii) The quartic Higgs self-coupling, which at the scale M_H is fixed by M_H itself, grows logarithmically with the energy scale. If M_H is small, the energy cut-off Λ at which the

coupling grows beyond any bound and new phenomena should occur, is large; if M_H is large, Λ is small. The condition $M_H \lesssim \Lambda$ sets an upper limit on the Higgs mass in the SM; lattice analyses lead to an estimate of about $M_H \sim 630$ GeV for this limit. Furthermore, top quark loops tend to drive the coupling to negative values for which the vacuum is no more stable. Therefore, requiring the SM to be extended to the GUT scale, $\Lambda_{\text{GUT}} \sim 10^{16}$ GeV, and including the effect of top quark loops on the running coupling, the Higgs mass should roughly lie in the range $130 \text{ GeV} \lesssim M_H \lesssim 180 \text{ GeV}$ [6]; see right panel of Fig. 1.

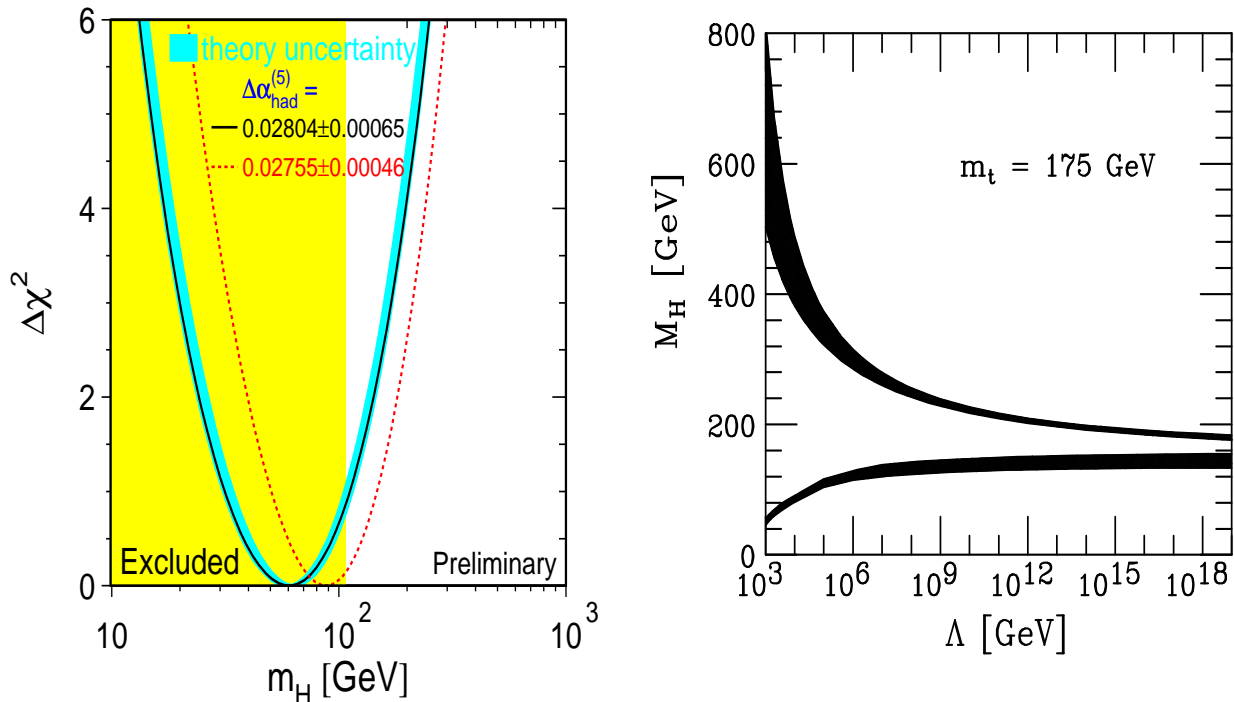


Figure 1: The χ^2 of the fit to electroweak data as a function of M_H (left) and triviality and vacuum stability bounds on M_H as a function of the new physics scale Λ (right).

However, there are two problems that one has to face when trying to extend the SM to Λ_{GUT} . The first one is the so-called hierarchy or naturalness problem: the Higgs boson tends to acquire a mass of the order of these large scales [the radiative corrections to M_H are quadratically divergent]; the second problem is that the simplest GUTs predict a value for $\sin^2 \theta_W$ that is incompatible with the measured value $\sin^2 \theta_W \simeq 0.23$. Low energy supersymmetry solves these two problems at once: supersymmetric particle loops cancel exactly the quadratic divergences and contribute to the running of the gauge coupling constants, correcting the small discrepancy to the observed value of $\sin^2 \theta_W$ [7].

The Minimal Supersymmetric extension of the Standard Model (MSSM) [7] requires the existence of two isodoublets of Higgs fields, to cancel anomalies and to give mass

separately to up and down-type fermions. Two CP-even neutral Higgs bosons h, H , a pseudoscalar A bosons and a pair of charged scalar particles, H^\pm , are introduced by this extension of the Higgs sector [2]. Besides the four masses, two additional parameters define the properties of these particles: a mixing angle α in the neutral CP-even sector and the ratio of the two vacuum expectation values $\tan\beta$, which from GUT restrictions is assumed in the range $1 \lesssim \tan\beta \lesssim m_t/m_b$ with the lower and upper ranges favored by Yukawa coupling unification [the lower range is excluded by LEP2 searches].

Supersymmetry leads to several relations among these parameters and only two of them, taken in general as M_A and $\tan\beta$ are in fact independent. These relations impose a strong hierarchical structure on the mass spectrum, $M_h < M_Z, M_A < M_H$ and $M_W < M_{H^\pm}$, which however is broken by radiative corrections if the top quark mass is large [8]. The leading part of this correction grows as the fourth power of m_t and logarithmically with the squark mass M_S ; the mixing (or trilinear coupling) in the stop sector A_t plays an important role. For instance, the upper bound on the mass of the lightest Higgs boson h is shifted from the tree level value M_Z to $M_h \sim 130$ GeV for $A_t = \sqrt{6}M_S$ with $M_S = 1$ TeV [8]. The masses of the heavy neutral and charged Higgs particles are expected to be in the range of the electroweak symmetry breaking scale; see left panel of Fig. 2.

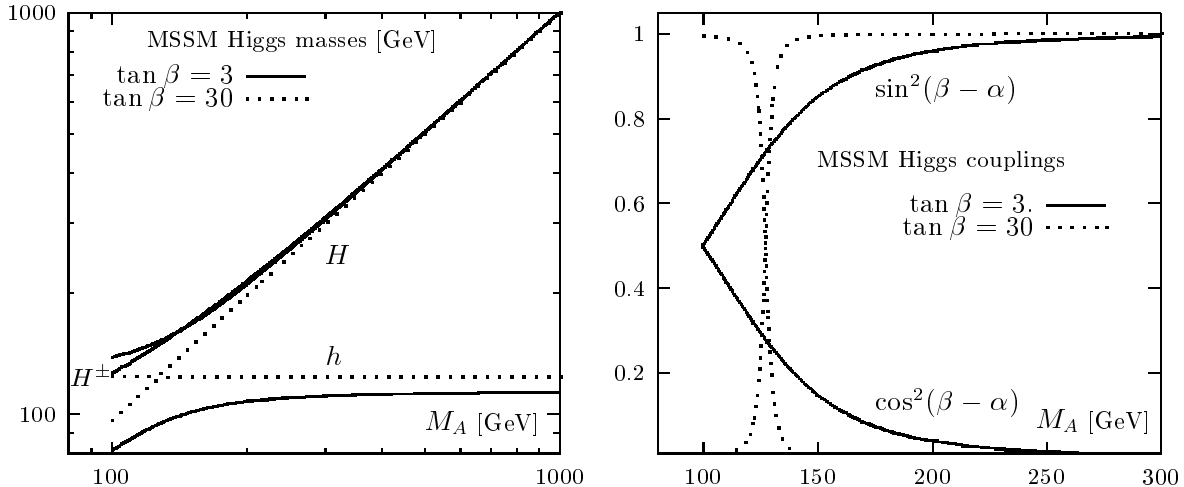


Figure 2: The masses of the Higgs bosons in the MSSM and their relative squared couplings to the massive gauge bosons for two representative values $\tan\beta=3$ and 30.

The couplings of the various neutral Higgs bosons [collectively denoted by Φ] to fermions and gauge bosons will in general strongly depend on the angles α and β ; normalized to the SM Higgs boson couplings, they are given by:

Φ	$g_{\Phi\bar{u}u}$	$g_{\Phi\bar{d}d}$	$g_{\Phi VV}$
h	$\cos\alpha/\sin\beta \rightarrow 1$	$-\sin\alpha/\cos\beta \rightarrow 1$	$\sin(\beta-\alpha) \rightarrow 1$
H	$\sin\alpha/\sin\beta \rightarrow 1/\tan\beta$	$\cos\alpha/\cos\beta \rightarrow \tan\beta$	$\cos(\beta-\alpha) \rightarrow 0$
A	$1/\tan\beta$	$\tan\beta$	0

The pseudoscalar has no tree level couplings to gauge bosons, and its couplings to down (up) type fermions are (inversely) proportional to $\tan\beta$. It is also the case for the couplings of the charged Higgs particle to fermions which are a mixture of scalar and pseudoscalar currents and depend only on $\tan\beta$. For the CP–even Higgs bosons, the couplings to down (up) type fermions are enhanced (suppressed) compared to the SM Higgs couplings for $\tan\beta > 1$. They share the SM Higgs couplings to vector bosons since they are suppressed by $\sin(\beta - \alpha)$ and $\cos(\beta - \alpha)$ factors, respectively for h and H ; see right panel of Fig. 2.

If the pseudoscalar mass is large, the h boson mass reaches its upper limit [which depends on the value of $\tan\beta$] and its couplings to fermions and gauge bosons are SM like; the heavier CP–even H and charged H^\pm bosons become degenerate with A . In this decoupling limit, it is very difficult to distinguish the Higgs sectors of the SM and MSSM.

Let us summarize the constraints on the MSSM Higgs particles masses, which mainly come from the negative LEP2 searches [3] in the Higgs–strahlung, $e^+e^- \rightarrow Z + h/H$, and pair production, $e^+e^- \rightarrow A + h/H$, processes which will be discussed in more detail later. In the decoupling limit where the h boson has SM–like couplings to Z bosons, the limit $M_h \gtrsim 114.1$ GeV from the $e^+e^- \rightarrow hZ$ process holds. This constraint rules out $\tan\beta$ values larger than $\tan\beta \gtrsim 3$. From the $e^+e^- \rightarrow Ah$ process, one obtains the absolute limits $M_h \gtrsim 91$ GeV and $M_A \gtrsim 92$ GeV, for a maximal ZhA coupling. In the general case, the allowed values for M_h are shown in Fig. 3 as a function of $\tan\beta$ (the colored regions) in the cases of maximal, typical and no–mixing in the stop sector, respectively $A_t = \sqrt{6}M_S, M_S$ and 0 for $M_S = 1$ TeV. Also are shown, the implications of the 2.1σ evidence for a SM–like Higgs boson with a mass $115.6_{-0.9}^{+1.3}$ GeV. Allowing for an error on the Higgs mass and an almost maximal coupling to the Z boson, the red (green) region indicates where $114 \text{ GeV} < M_h(M_H) < 117 \text{ GeV}$ and $\sin(\cos)^2(\beta - \alpha) > 0.9$.

In more general SUSY scenarii, one can add an arbitrary number of Higgs doublet and/or singlet fields without being in conflict with high precision data [4]. The Higgs spectrum becomes then much more complicated than in the MSSM, and much less constrained. However, the triviality argument always imposes a bound on the mass of the lightest Higgs boson of the theory. For instance, if only one Higgs singlet field is added to the MSSM, an upper bound $M_h \lesssim 150$ GeV can be set [9]. In the most general SUSY model, with arbitrary matter content and gauge coupling unification near Λ_{GUT} , and absolute upper limit on the mass of the lightest Higgs boson, $M_h \lesssim 205$ GeV, has been derived [10].

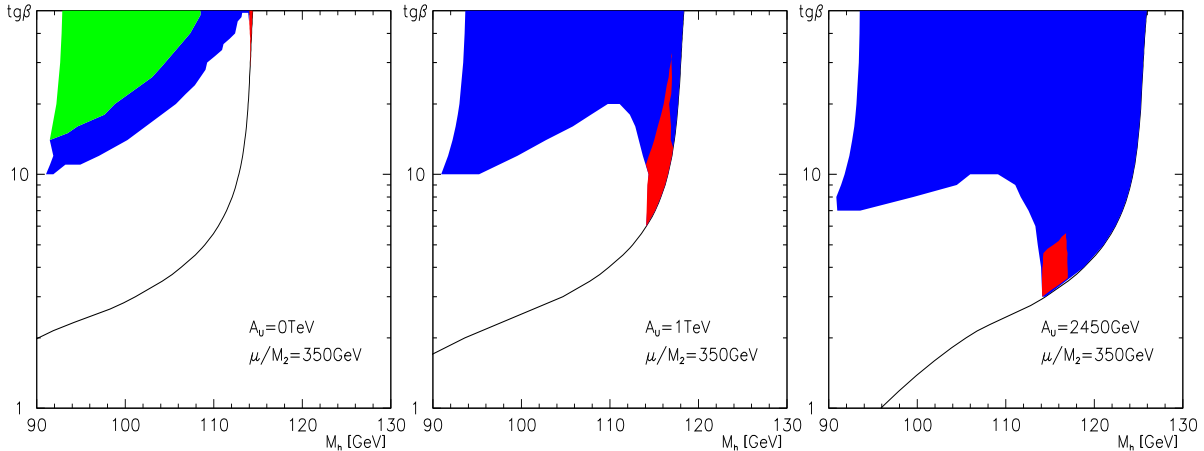


Figure 3: The allowed (colored) regions for M_h from LEP2 searches as a function of $\tan\beta$ in the case of maximal, typical and no stop mixing; From Ref. [7].

Thus, either in the SM or in its SUSY extensions, a Higgs boson should be lighter than ~ 200 GeV, and will be therefore kinematically accessible at the next generation of experiments. In the following, after summarizing the decay modes of the Higgs bosons, I will briefly discuss the discovery potential of present and future colliders, the Tevatron Run II [12], the LHC [13, 14] and a future e^+e^- linear collider [15] with a c.m. energy in the range of 300 to 800 GeV such as the TESLA machine [16].

2. Decay Modes

Let us first discuss the Higgs decay modes relying on the analyses of Ref. [17]; see Fig. 4. To simplify the discussion in the SM, it is convenient to divide the Higgs mass into two ranges: the “low mass” range $M_H \lesssim 130$ GeV and the “high mass” range $M_H \gtrsim 130$ GeV.

In the “low mass” range, the Higgs boson decays into a large variety of channels. The main decay mode is by far the decay into $b\bar{b}$ pairs with a branching ratio of $\sim 90\%$ followed by the decays into $c\bar{c}$ and $\tau^+\tau^-$ pairs with branching ratios of $\sim 5\%$. Also of significance, the top-loop mediated Higgs decay into gluons, which for M_H around 120 GeV occurs at the level of $\sim 5\%$. The top and W -loop mediated $\gamma\gamma$ and $Z\gamma$ decay modes are very rare the branching ratios being of $\mathcal{O}(10^{-3})$. However, these decays lead to clear signals and are theoretically interesting being sensitive to new heavy particles such as SUSY particles.

In the “high mass” range, the Higgs bosons decay into WW and ZZ pairs, with one of the gauge bosons being virtual below the threshold. Above the ZZ threshold, the Higgs boson decays almost exclusively into these channels with a branching ratio of $2/3$ for WW and $1/3$ for ZZ . The opening of the $t\bar{t}$ channel does not alter significantly this pattern.

In the low mass range, the Higgs boson is very narrow $\Gamma_H < 10$ MeV, but the width

becomes rapidly wider for masses larger than 130 GeV, reaching 1 GeV at the ZZ threshold. The Higgs total width cannot be measured directly in the mass range below 250 GeV. For large masses, $M_H \gtrsim 500$ GeV, the Higgs boson becomes obese since its total width is comparable to its mass, and it is hard to consider the Higgs as a resonance.

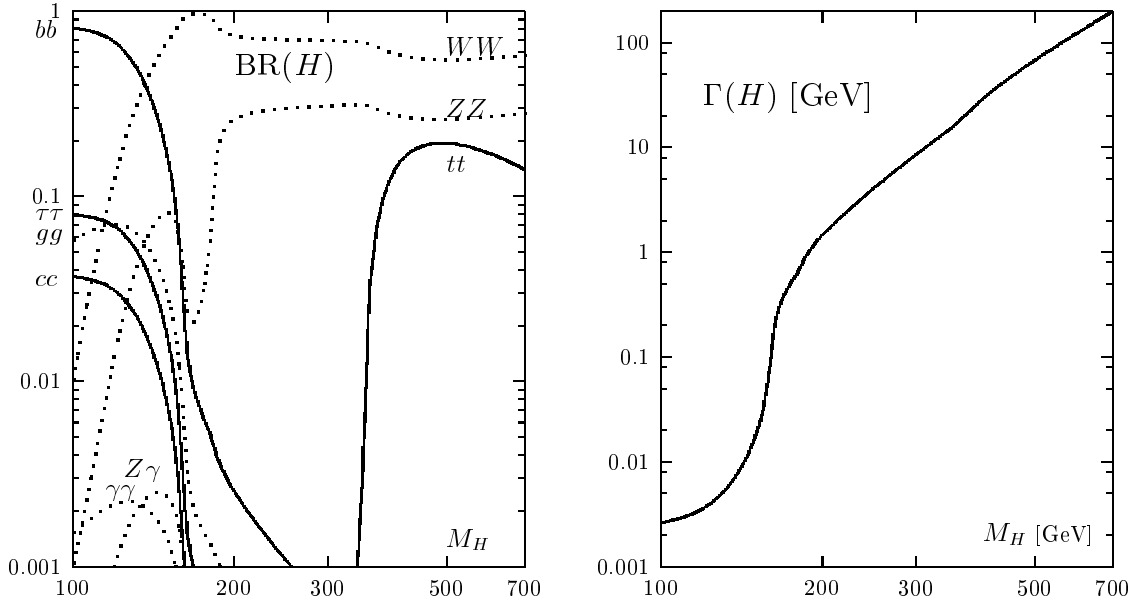


Figure 4: The decay branching ratios (left) and the total decay width (right) of the SM Higgs boson as a function of its mass.

The decay pattern of the Higgs bosons of the MSSM [17] is more complicated than in the SM and depends strongly on the value of $\tan\beta$; see Fig. 5.

The lightest h boson will decay mainly into fermion pairs since its mass is smaller than ~ 130 GeV. This is, in general, also the dominant decay mode of the pseudoscalar boson A . For values of $\tan\beta$ much larger than unity, the main decay modes of the three neutral Higgs bosons are decays into $b\bar{b}$ and $\tau^+\tau^-$ pairs with the branching ratios being of order $\sim 90\%$ and 10% , respectively. For large masses, the top decay channels $H, A \rightarrow t\bar{t}$ open up, yet for large $\tan\beta$ these modes remain suppressed. If the masses are high enough, the heavy H boson can decay into gauge bosons or light h boson pairs and the pseudoscalar A particle into hZ final states. However, these decays are strongly suppressed for $\tan\beta \gtrsim 3-5$ as is suggested by the LEP2 constraints.

The charged Higgs particles decay into fermions pairs: mainly $t\bar{b}$ and $\tau\nu_\tau$ final states for H^\pm masses, respectively, above and below the $t\bar{b}$ threshold. If allowed kinematically and for small values of $\tan\beta$, the H^\pm bosons decay also into hW final states for $\tan\beta \lesssim 5$.

Adding up the various decay modes, the widths of all five Higgs bosons remain very narrow. The total width of one the CP-even Higgs particle will be close to the SM Higgs

width, while the total widths of the other Higgs particles will be proportional to $\tan\beta$ and will be of the order of 10 GeV even for large masses.

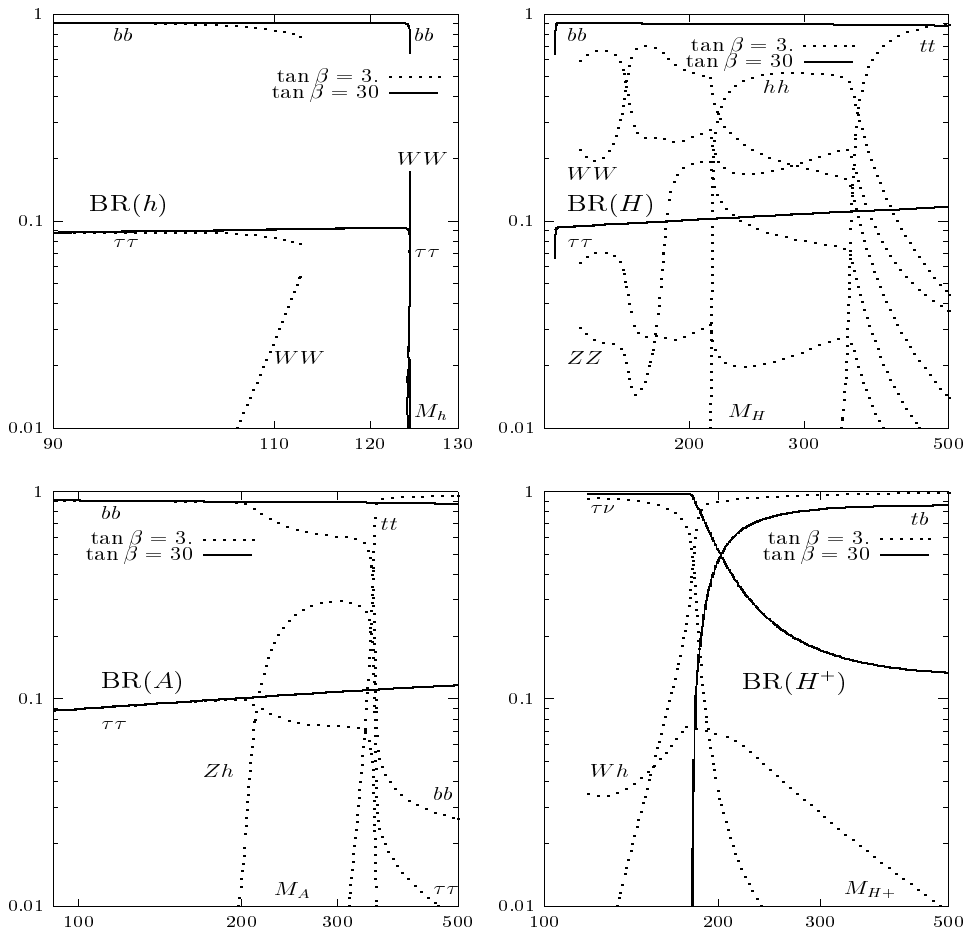


Figure 5: Dominant MSSM Higgs bosons decay branching ratios as functions of the Higgs boson masses for $\tan\beta = 3$ and 30.

Other possible decay channels for the MSSM bosons, in particular the heavy H , A and H^\pm states, are decays into supersymmetric particles [18]. In addition to light sfermions, decays into charginos and neutralinos could eventually be important if not dominant. Decays of the lightest h boson into the lightest neutralinos (LSP) or sneutrinos can be also important, exceeding 50% in some parts of the SUSY parameter space. These decays can render the search for Higgs particle rather difficult, in particular at hadron colliders.

In more general SUSY scenarii, the decays of the Higgs bosons can be much more complicated than in the MSSM. In particular decays of the heavy Higgses into gauge bosons and cascade decays into lighter Higgs bosons are still allowed. This might render the search strategies of these particles complicated at the LHC. At e^+e^- colliders however, this does not lead to any difficulty to detect some of the particles as will be discussed later.

3. Higgs Production at Hadron Colliders

The main production mechanisms of neutral Higgs bosons in the SM at hadron colliders are the following processes [19]

- | | | |
|-----|-----------------------------|---|
| (a) | gluon – gluon fusion | $gg \rightarrow H$ |
| (b) | WW/ZZ fusion | $VV \rightarrow H$ |
| (c) | association with W/Z | $q\bar{q} \rightarrow V + H$ |
| (d) | association with $Q\bar{Q}$ | $gg, q\bar{q} \rightarrow Q\bar{Q} + H$ |

The cross sections are shown in Fig. 6 for the LHC with $\sqrt{s} = 14$ TeV and for the Tevatron with $\sqrt{s} = 2$ TeV as functions of the Higgs boson masses; from Ref. [20].

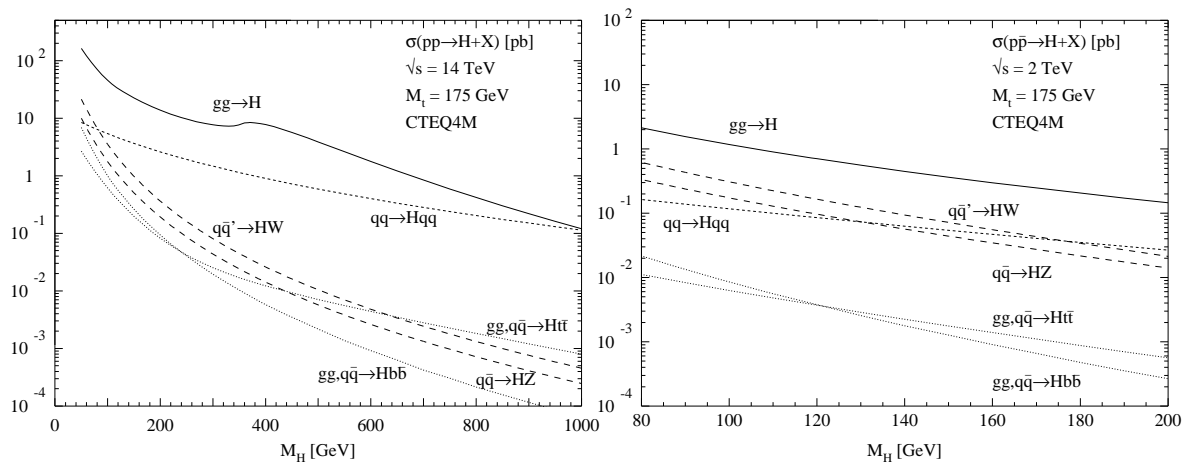


Figure 6: Higgs boson production cross sections at the LHC (left) and the Tevatron (right) for the various mechanisms as functions of the Higgs mass.

At the LHC, in the interesting mass range $100 \text{ GeV} \lesssim M_H \lesssim 250 \text{ GeV}$, the dominant production process of the SM Higgs boson is by far the gluon–gluon fusion mechanism [in fact it is the case of the entire Higgs mass range] the cross section being of the order a few tens of pb. It is followed by the WW/ZZ fusion processes with a cross section of a few pb [which reaches the level of gg fusion for very large M_H]. The cross sections of the associated production with W/Z bosons or $t\bar{t}$, $b\bar{b}$ pairs are one to two orders of magnitude smaller than the gg cross section. Note that for an integrated luminosity $\int \mathcal{L} = (10) 100 \text{ fb}^{-1}$ in the low (high) luminosity option, $\sigma = 1 \text{ pb}$ would correspond to $10^4(10^5)$ events.

At the Tevatron, the most relevant production mechanism is the associated production with W/Z bosons, where the cross section is slightly less than a picobarn for $M_H \sim 120 \text{ GeV}$, leading to $\sim 10^4$ Higgs events for a luminosity $\int \mathcal{L} = 20 \text{ fb}^{-1}$. The WW/ZZ fusion cross sections are slightly smaller for $M_H \lesssim 150 \text{ GeV}$, while the cross sections for associated production with $t\bar{t}$ or $b\bar{b}$ pairs are rather low. The gg fusion mechanism has the largest cross section but suffers from a huge QCD two–jet background.

The next-to-leading order QCD corrections should be taken into account in the gg fusion processes where they are large, leading to an increase of the production cross sections by a factor of up to two [21]. For the other processes, the QCD radiative corrections are relatively smaller [22]: for the associated production with gauge bosons, the corrections [which can be inferred from the Drell–Yan W/Z production] are at the level of 10%, while in the case of the vector boson fusion processes, they are at the level of 30%. For the associated production with top quarks, the NLO corrections alter the cross section by $\sim 20\%$ if the scale is chosen properly. In all these production processes, the theoretical uncertainty, from the remaining scale dependence and from the choice of different sets of parton densities, can be estimated as being of the order of $\sim 20\text{--}30\%$.

The signals which are best suited to identify the produced Higgs particles at the Tevatron and at the LHC have been studied in great detail in Refs. [12, 13], respectively. I briefly summarize below the main conclusions of these studies.

At the Tevatron Run II, the associated production with W/Z bosons with the latter decaying leptonically lead to several distinct signatures in which a signal can be observed with sufficient integrated luminosity. In the low Higgs mass range, $M_H \lesssim 130$ GeV, the Higgs will mainly decay into $b\bar{b}$ pairs and the most sensitive signatures are $\ell\nu b\bar{b}$, $\nu\bar{\nu}b\bar{b}$, and $\ell^+\ell^-b\bar{b}$. Hadronic decays of the W and Z lead to the $q\bar{q}b\bar{b}$ final state and cannot be used since they suffer from large backgrounds from QCD multi-jet production. In the high Higgs mass range, $M_H \gtrsim 130$ GeV, the dominant decay is $H \rightarrow WW^*$ and the signature $\ell^\pm\ell^\pm jj$ from three vector boson final states can be used. In addition, one can use the final state $\ell^+\ell^-\nu\bar{\nu}$ with the Higgs boson produced in gg fusion.

The required luminosity to discover or exclude a SM Higgs boson, combining all channels in both D0 and CDF experiments, is shown in Fig. 7 as a function of M_H [12]. With 15 fb^{-1} luminosity, a 5σ signal can be achieved for $M_H \lesssim 120$ GeV, while a Higgs boson with a mass $M_H \lesssim 190$ GeV can be excluded at the 95% confidence level.

Let us now turn to the signatures which can be used at the LHC. A discovery with a significance larger than 5σ can be obtained using various channels; see Figure 8.

In the high mass range, $M_H \gtrsim 130$ GeV, the signal consists of the so-called “gold-plated” events $H \rightarrow ZZ^{(*)} \rightarrow 4\ell^\pm$ with $\ell = e, \mu$. The backgrounds, mostly $pp \rightarrow ZZ^{(*)}, Z\gamma^*$ for the irreducible background and $t\bar{t} \rightarrow WWb\bar{b}$ and $Zb\bar{b}$ for the reducible one, are relatively small. One can probe Higgs boson masses up to $\mathcal{O}(500 \text{ GeV})$ with a luminosity $\int \mathcal{L} = 100 \text{ fb}^{-1}$. The channels $H \rightarrow ZZ \rightarrow \nu\bar{\nu}\ell^+\ell^-$ and $H \rightarrow WW \rightarrow \nu\ell jj$, which have larger rates, allow to extend the reach to $M_H \sim 1 \text{ TeV}$. The $H \rightarrow WW^{(*)} \rightarrow \nu\bar{\nu}\ell^+\ell^-$ [with H produced in gg fusion, and to a lesser extent, in association with W bosons] decay channel is very useful in the range $130 \text{ GeV} \lesssim M_H \lesssim 180 \text{ GeV}$, where $\text{BR}(H \rightarrow ZZ^*)$ is too small, despite of the large background from WW and $t\bar{t}$ production.

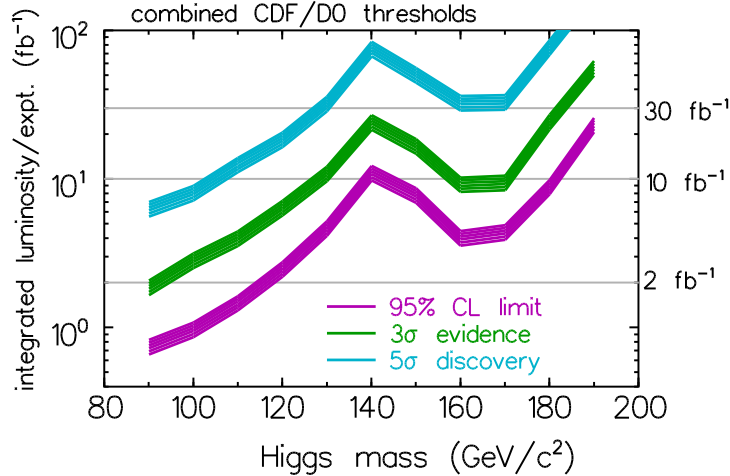


Figure 7: The integrated luminosity required per experiment, to either exclude a SM Higgs boson at 95% CL or discover it at the 3σ or 5σ level, as a function of M_H .

For the “low mass” range, the situation is more complicated. The branching ratios for $H \rightarrow ZZ^*, WW^*$ are too small and due to the huge QCD jet background, the dominant mode $H \rightarrow b\bar{b}$ is practically useless. One has then to rely on the rare $\gamma\gamma$ decay mode with a branching ratio of $\mathcal{O}(10^{-3})$, where the Higgs boson is produced in the gg fusion and the associated WH and $Ht\bar{t}$ processes. A 5σ discovery can be obtained with a luminosity $\int \mathcal{L} = 100 \text{ fb}^{-1}$, despite of the formidable backgrounds. Finally, in the very low mass range, $M_H \sim 115 \text{ GeV}$, the channel $pp \rightarrow t\bar{t}H$ with $H \rightarrow b\bar{b}$ can be used.

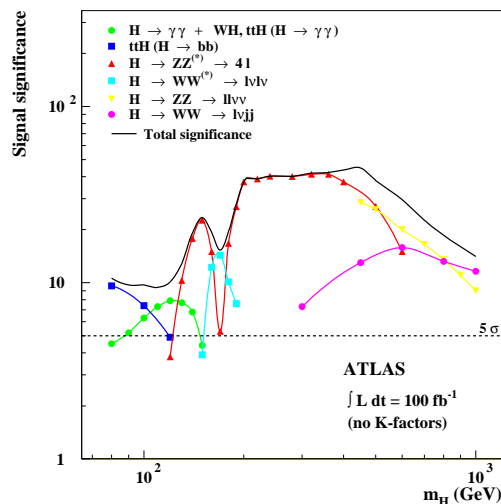


Figure 8: Significance for the SM Higgs boson discovery in various channels at the LHC with a high luminosity as a function of the Higgs mass.

In the MSSM, the production processes for the neutral CP–even Higgs particles are practically the same as for the SM Higgs. However, for large $\tan\beta$ values, one has to take the b quark [whose couplings are strongly enhanced] into account: its loop contributions in the gg fusion process [and also the extra contributions from squarks loops, which however decouple for high squark masses] and associated production with $b\bar{b}$ pairs. The cross sections for the associated production with $t\bar{t}$ pairs and W/Z bosons and the WW/ZZ fusion processes, are suppressed for at least one of the particles because of the coupling suppression. Because of CP–invariance, the pseudoscalar A boson can be produced only in the gg fusion and in association with heavy quarks [associated production with a CP–even Higgs particle, $pp \rightarrow A + h/H$, is also possible but the cross section is too small]. For high enough $\tan\beta$ values and for $M_A \gtrsim (\lesssim) 130$ GeV, the $gg/q\bar{q} \rightarrow b\bar{b} + A/H(h)$ and $gg \rightarrow A/H(h)$ processes become the dominant production mechanisms.

The charged Higgs particles, if lighter than the top quark, can be accessible in the decays $t \rightarrow H^+b$ with $H^- \rightarrow \tau\nu_\tau$, leading to a surplus of τ events mimicking a breaking of τ versus e, μ universality. The H^\pm particles can also be produced directly in the [properly combined] processes $gb \rightarrow tH^-$ or $qq/gg \rightarrow H^-t\bar{b}$.

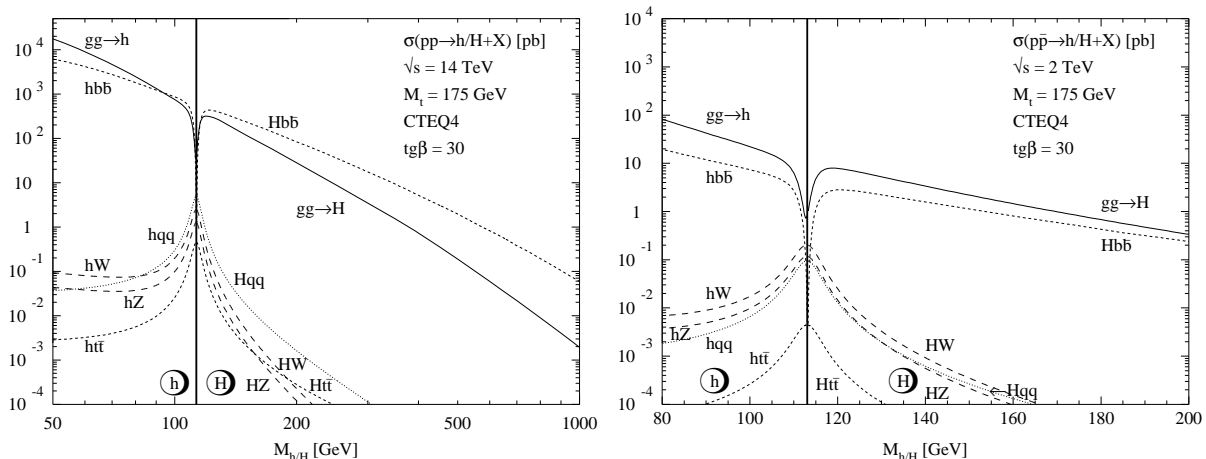


Figure 9: CP–even Higgs production cross sections at LHC (left) and Tevatron (right) for the various mechanisms as a function of the Higgs masses for $\tan\beta = 30$.

The cross sections for the production of the CP–even Higgs particles are shown in Fig. 9 for the Tevatron and LHC for $\tan\beta = 30$ [the cross sections for A production are roughly equal to the one of the $h(H)$ particle in the low (high) mass range]; from Ref. [20]. The various detection signals can be briefly summarized as follows [see also Fig. 10]:

(i) Since the lightest Higgs boson mass is always smaller than ~ 130 GeV, the WW and ZZ signals cannot be used. Furthermore, the $hWW(h\bar{b}b)$ coupling is suppressed (enhanced) leading to a smaller $\gamma\gamma$ branching ratio than in the SM, making the search in this channel more difficult. If M_h is close to its maximum value, h has SM like couplings and the situation is similar to the SM case with $M_H \sim 100\text{--}130$ GeV.

(ii) Since A has no tree-level couplings to gauge bosons and since the couplings of H are strongly suppressed, the gold-plated ZZ signal is lost [for H it survives only for small $\tan\beta$ values, provided that $M_H < 2m_t$]. In addition, the $A/H \rightarrow \gamma\gamma$ signals cannot be used since the branching ratios are suppressed. One has then to rely on the $A/H \rightarrow \tau^+\tau^-$ or even $\mu^+\mu^-$ channels for large $\tan\beta$ values. [The decays $H \rightarrow hh \rightarrow b\bar{b}b\bar{b}$, $A \rightarrow hZ \rightarrow Zb\bar{b}$ and $H/A \rightarrow t\bar{t}$ have too small rates in view of the LEP2 constraints].

(iii) Light H^\pm particles can be observed in the decays $t \rightarrow H^+b$ with $H^- \rightarrow \tau\nu_\tau$ where masses up to ~ 150 GeV can be probed. The mass reach can be extended up to a few hundred GeV for $\tan\beta \gg 1$, by considering the processes [23] $gb \rightarrow tH^-$ and $gg \rightarrow t\bar{b}H^-$ with the decays $H^- \rightarrow \tau\nu_\tau$ [using τ polarization] or $\bar{t}b$.

(iv) All the previous discussion assumes that Higgs decays into SUSY particles are kinematically inaccessible. This seems to be unlikely since at least the decays of the heavier H, A and H^\pm particles into charginos and neutralinos should be possible [18]. Preliminary analyses show that decays into neutralino/chargino final states $H/A \rightarrow \chi_2^0\chi_2^0 \rightarrow 4\ell^\pm X$ and $H^\pm \rightarrow \chi_2^0\chi_1^\pm \rightarrow 3\ell^\pm X$ can be detected in some cases [24]. It could also be possible that the lighter h decays invisibly into the lightest neutralinos or sneutrinos. If this scenario is realized, the discovery of these Higgs particles will be more challenging. Preliminary analyses for the 2001 les Houches Workshop in Ref. [13] show however, that an invisibly decaying Higgs boson could be detected in the WW fusion process.

(v) If top squarks are light enough, their contribution to the gg fusion mechanism and to the $\gamma\gamma$ decay [here, this is also the case for light charginos] should be taken into account. In the large mixing scenario, stops can be rather light and couple strongly to the h boson, leading to a possibly strong suppression of the product $\sigma(gg \rightarrow h) \times \text{BR}(h \rightarrow \gamma\gamma)$ [25]. However, in this case, the associated production of the h boson with top squarks is possible and the cross sections would be rather sizeable [26].

(vi) MSSM Higgs boson detection from the cascade decays of Supersymmetric particles, originating from squark and gluino production, are also possible. In particular, the production of the lighter h boson from the decays of the next-to-lightest neutralino and the production of H^\pm from the decays of the heavier chargino/neutralino states into the lighter ones have been discussed; see Ref. [27] for instance.

At the Tevatron Run II, the search for the CP-even h and H bosons will be more difficult than in the SM because of the reduced couplings to gauge bosons, unless one of the Higgs particles is SM-like. However, associated production with $b\bar{b}$ pairs, $pp \rightarrow b\bar{b} + A/h(H)$ in the low (high) M_A range with the Higgs bosons decaying into $b\bar{b}$ pairs, might lead to a visible signal for rather large $\tan\beta$ values and M_A values below the 200 GeV range. The H^\pm boson would be also accessible in top quark decays for large or small values of $\tan\beta$, for which the branching ratio $\text{BR}(t \rightarrow H^+b)$ is large enough,

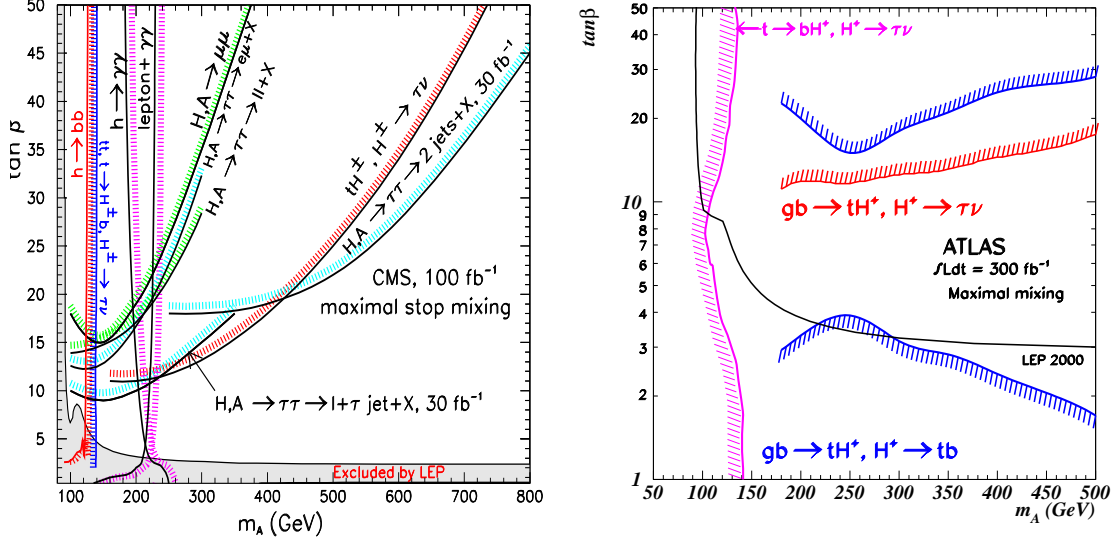


Figure 10: Neutral (left) and charged (right) MSSM Higgs boson discovery at the LHC in various channels in the $(M_A, \tan \beta)$ plane with a high luminosity.

In more general SUSY extensions of the SM, the Higgs spectrum can be much more complicated than in the MSSM. While the production mechanisms will probably remain the same, the production cross sections can be different. The decay signatures could also be much more complicated than in the MSSM. This would make the search for the Higgs bosons of these extensions very challenging. There are no detailed simulations which have been performed on this issue yet. A preliminary theoretical analysis [28] in the context of the NMSSM, i.e. the MSSM supplemented by one Higgs singlet, has been devoted to the observability of at least one Higgs boson at the LHC with 300 fb^{-1} integrated luminosity, taking the present LEP2 constraints into account and making use of the WW fusion mechanism. It concludes that the LHC will discover at least one NMSSM Higgs boson unless there are large branching ratios for decays to SUSY particles and/or to other Higgs bosons. This analysis needs to be confirmed by detailed (experimental) simulations.

4. Higgs Production at e^+e^- Colliders

At e^+e^- linear colliders operating in the 300–800 GeV energy range, the main production mechanisms for SM-like Higgs particles are [29]

- | | | |
|-----|------------------------|---|
| (a) | bremsstrahlung process | $e^+e^- \rightarrow (Z) \rightarrow Z + H$ |
| (b) | WW fusion process | $e^+e^- \rightarrow \bar{\nu} \nu (WW) \rightarrow \bar{\nu} \nu + H$ |
| (c) | ZZ fusion process | $e^+e^- \rightarrow e^+e^- (ZZ) \rightarrow e^+e^- + H$ |
| (d) | radiation off tops | $e^+e^- \rightarrow (\gamma, Z) \rightarrow t\bar{t} + H$ |

The Higgs–strahlung cross section scales as $1/s$ and therefore dominates at low energies while the WW fusion mechanism has a cross section which rises like $\log(s/M_H^2)$ and dominates at high energies. At $\sqrt{s} \sim 500$ GeV, the two processes have approximately the same cross sections, $\mathcal{O}(100 \text{ fb})$ for the interesting range $100 \text{ GeV} \lesssim M_H \lesssim 200 \text{ GeV}$, as shown in Fig. 11. With an integrated luminosity $\int \mathcal{L} \sim 500 \text{ fb}^{-1}$, as expected for instance at the TESLA machine [16], approximately 25.000 events per year can be collected in each channel for a Higgs boson with a mass $M_H \sim 150$ GeV. This sample is more than enough to discover the Higgs boson and to study its properties in detail.

The ZZ fusion mechanism has a cross section which is one order of magnitude smaller than WW fusion, a result of the smaller neutral couplings compared to charged current couplings. The associated production with top quarks has a very small cross section at $\sqrt{s} = 500$ GeV due to the phase space suppression but at $\sqrt{s} = 1$ TeV it can reach the level of a few femtobarn. Despite of the small production cross sections, shown in Fig. 11 as a function of \sqrt{s} for $M_H = 120$ GeV, these processes will be very useful when it comes to study the Higgs properties as will be discussed later. The cross section for the double Higgs production in the strahlung process [30], $e^+e^- \rightarrow HHZ$, also shown in Fig. 11 is at the level of a fraction of a femtobarn and can be used to extract the Higgs self–coupling.

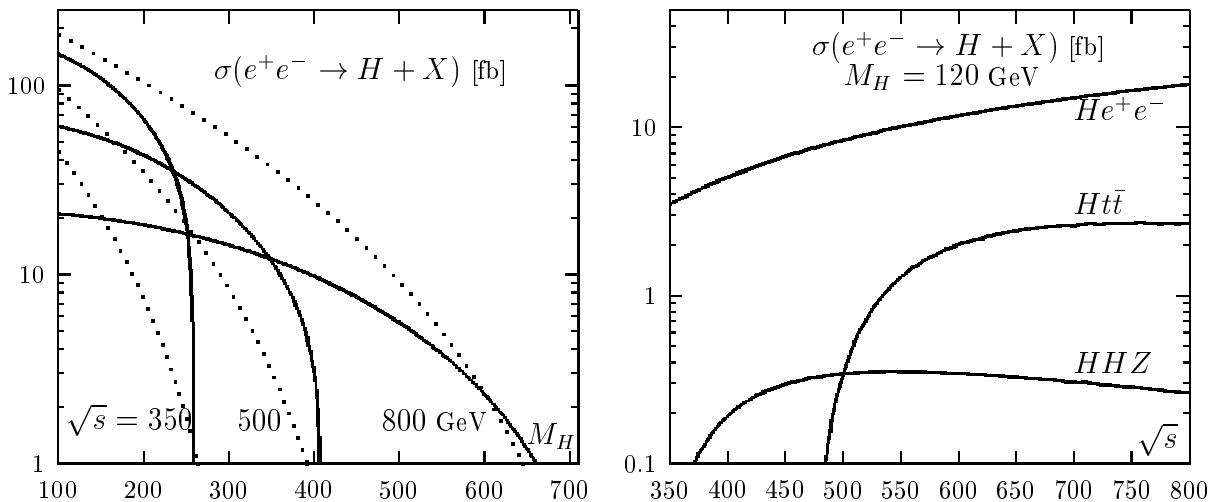


Figure 11: Production cross sections of the SM Higgs boson in e^+e^- in the main processes with $\sqrt{s} = 350, 500$ and 800 GeV as a function of M_H (left) and in higher order process as a function of \sqrt{s} for $M_H = 120$ GeV (right).

In the Higgs–strahlung process, the recoiling Z boson [which can be tagged through its clean $\mu^+\mu^-$ decay] is mono–energetic and M_H can be derived from the energy of the Z if the initial e^+ and e^- beam energies are sharp [beamstrahlung, which smears out the c.m. energy should thus be suppressed as strongly as possible, and this is already the case for machine designs such as TESLA]. Therefore, it will be easy to separate the signal from the backgrounds. For low Higgs masses, $M_H \lesssim 130$ GeV, the main background will

be $e^+e^- \rightarrow ZZ$. The cross section is large, but it can be reduced by cutting out the forward and backward directions [the process is mediated by t -channel e exchange] and by selecting $b\bar{b}$ final states by means of μ -vertex detectors [while the Higgs decays almost exclusively into $b\bar{b}$ in this mass range, $\text{BR}(Z \rightarrow b\bar{b})$ is small, $\sim 15\%$]. The background from single Z production, $e^+e^- \rightarrow Zq\bar{q}$, is small and can be further reduced by flavor tagging. In the mass range where the decay $H \rightarrow WW^*$ is dominant, the main background is triple gauge boson production and is suppressed by two powers of the electroweak coupling.

The WW fusion mechanism offers a complementary production channel. For small M_H , the main backgrounds are single W production, $e^+e^- \rightarrow e^\pm W^\mp \nu$ [$W \rightarrow q\bar{q}$ and the e^\pm escape detection] and WW fusion into a Z boson, $e^+e^- \rightarrow \nu\bar{\nu}Z$, which have cross sections 60 and 3 times larger than the signal, respectively. Cuts on the rapidity spread, the energy and momentum distribution of the two jets in the final state [as well as flavor tagging for small M_H] will suppress these background events.

It has been shown in detailed simulations [16] that only a few fb^{-1} of integrated luminosity are needed to obtain a 5σ signal for a Higgs boson with a mass $M_H \lesssim 140$ GeV at a 500 GeV collider [in fact, in this case, it is better to go to lower energies where the cross section is larger], even if it decays invisibly [as it could happen in SUSY models for instance]. Higgs bosons with masses up to $M_H \sim 400$ GeV can be discovered at the 5σ level, in both the strahlung and fusion processes at an energy of 500 GeV and with a luminosity of 500 fb^{-1} . For even higher masses, one needs to increase the c.m. energy of the collider, and as a rule of thumb, Higgs masses up to $\sim 80\%\sqrt{s}$ can be probed. This means that a ~ 1 TeV collider will be needed to probe the entire SM Higgs mass range.

An even stronger case for e^+e^- colliders in the 300–800 GeV energy range is made by the MSSM. In e^+e^- collisions [31], besides the usual bremsstrahlung and fusion processes for h and H production, the neutral Higgs particles can also be produced pairwise: $e^+e^- \rightarrow A + h/H$. The cross sections for the bremsstrahlung and the pair production as well as the cross sections for the production of h and H are mutually complementary, coming either with a coefficient $\sin^2(\beta - \alpha)$ or $\cos^2(\beta - \alpha)$; see Fig. 12. The cross section for hZ production is large for large values of M_h , being of $\mathcal{O}(100 \text{ fb})$ at $\sqrt{s} = 350$ GeV; by contrast, the cross section for HZ is large for light h [implying small M_H]. In major parts of the parameter space, the signals consist of a Z boson and $b\bar{b}$ or $\tau^+\tau^-$ pairs, which is easy to separate from the main background, $e^+e^- \rightarrow ZZ$ [in particular with b -tagging]. For the associated production, the situation is opposite: the cross section for Ah is large for light h whereas AH production is preferred in the complementary region. The signal consists mostly of four b quarks in the final state, requiring efficient $b\bar{b}$ quark tagging; mass constraints help to eliminate the QCD jets and ZZ backgrounds. The CP-even Higgs particles can also be searched for in the WW and ZZ fusion mechanisms.

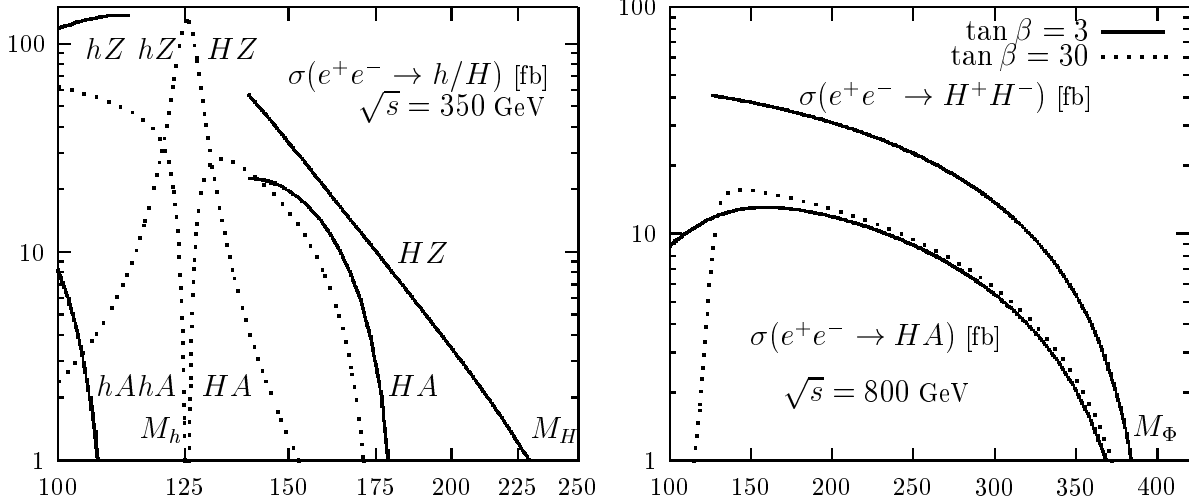


Figure 12: Production cross sections of the MSSM Higgs bosons in e^+e^- as functions of the masses: h, H production at $\sqrt{s} = 350$ GeV (left) and HA, H^+H^- production at $\sqrt{s} = 800$ GeV (right); the dotted (full) lines are for $\tan\beta = 30(3)$.

In e^+e^- collisions, charged Higgs bosons can be produced pairwise, $e^+e^- \rightarrow H^+H^-$, through γ, Z exchange. The cross section depends only on the charged Higgs mass; it is large almost up to $M_{H^\pm} \sim \sqrt{s}/2$. H^\pm bosons can also be produced in top decays as at hadron colliders; in the range $1 < \tan\beta < m_t/m_b$, the $t \rightarrow H^+b$ branching ratio and the $t\bar{t}$ production cross sections are large enough to allow for their detection in this mode.

The discussion on the MSSM Higgs production at e^+e^- linear colliders [not mentioning yet the $\gamma\gamma$ option of the collider] can be summarized in the following points [16]:

i) The Higgs boson h can be detected in the entire range of the MSSM parameter space, either through the bremsstrahlung process or pair production; in fact, this conclusion holds true even at a c.m. energy of 300 GeV and with a luminosity of a few fb^{-1} .

ii) All SUSY Higgs bosons can be discovered at an e^+e^- collider if the H, A and H^\pm masses are less than the beam energy; for higher masses, one simply has to increase \sqrt{s} .

iii) Even if the decay modes of the Higgs bosons are very complicated [e.g. they decay invisibly] missing mass techniques allow for their detection.

iv) The additional associated production processes with $t\bar{t}$ and $b\bar{b}$ allow for the measurement of the Yukawa couplings. In particular, $e^+e^- \rightarrow b\bar{b} + H/A$ for high $\tan\beta$ values allows for the determination of this important parameter for low M_A values [32].

In extensions of the MSSM, the Higgs production processes are as the ones above but the phenomenological analyses are more involved since there is more freedom in the choice of parameters. However, even if the Higgs sector is extremely complicated, there is always a light Higgs boson which has sizeable couplings to the Z boson. This Higgs particle can be thus produced in the strahlung process, $e^+e^- \rightarrow Z + "h"$, and using the missing mass technique this "h" particle can be detected. Recently a "no-loose theorem" has been

proposed [33]: a Higgs boson in SUSY theories can be always detected at a 500 GeV e^+e^- collider with a luminosity of $\int \mathcal{L} \sim 500 \text{ fb}^{-1}$ in the strahlung process, regardless of the complexity of the Higgs sector of the theory and of the decays of the Higgs boson.

Finally, future linear colliders can be turned to $\gamma\gamma$ colliders, in which the photon beams are generated by Compton back-scattering of laser light; c.m. energies of the order of 80% of the e^+e^- collider energy and integrated luminosities $\int \mathcal{L} \sim 100 \text{ fb}$, as well as a high degree of longitudinal photon polarization can be reached at these colliders [34].

Tuning the maximum of the $\gamma\gamma$ spectrum to the value of the Higgs boson mass, the Higgs particles can be formed as s -channel resonances, $\gamma\gamma \rightarrow \text{Higgs}$, decaying mostly into $b\bar{b}$ pairs [35]. The main background, $\gamma\gamma \rightarrow b\bar{b}$, can be suppressed by choosing proper helicities for the initial e^\pm and laser photons which maximizes the signal cross section, and eliminating the gluon radiation by taking into account only two-jet events. Clear signals can be obtained which allow the measurement of the Higgs couplings to photons, which are mediated by loops possibly involving new particles. In addition, in the MSSM, $\gamma\gamma$ colliders allow to extend the reach for the heavy H, A bosons compared to the e^+e^- option [36].

5. Determination of the properties of a SM-like Higgs boson

Once the Higgs boson is found it will be of great importance to explore all its fundamental properties. This can be done at great details in the clean environment of e^+e^- linear colliders [16, 37]: the Higgs mass, the spin and parity quantum numbers and the couplings to fermions, gauge bosons and the self-couplings can be measured. Some precision measurements, in particular for the mass and width, can also be performed at the LHC with high-luminosity [13, 14, 38]. In the following we will summarize these features in the case of the SM Higgs boson; some of this discussion can be of course extended to the lightest MSSM Higgs particle. We will rely on Refs. [14, 38] and [16, 37] for the LHC and TESLA analyses, respectively, where the references for the original studies can be found.

5.1 Studies at e^+e^- Colliders

- The measurement of the recoil e^+e^- or $\mu^+\mu^-$ mass in the Higgs-strahlung process, $e^+e^- \rightarrow ZH \rightarrow He^+e^-$ and $H\mu^+\mu^-$, allows a very good determination of the Higgs boson mass. At $\sqrt{s} = 350 \text{ GeV}$ and with a luminosity of $\int \mathcal{L} = 500 \text{ fb}^{-1}$, a precision of $\Delta M_H \sim 70 \text{ MeV}$ can be reached for a Higgs boson mass of $M_H \sim 120 \text{ GeV}$. The precision can be increased to $\Delta M_H \sim 40 \text{ MeV}$ by using in addition the hadronic decays of the Z boson [which have more statistics]. Accuracies of the order of $\Delta M_H \sim 80 \text{ MeV}$ can also be reached for $M_H = 150$ and 180 GeV when the Higgs decays mostly into gauge bosons.

This one per mile accuracy on M_H can be very important, especially in the MSSM where it allow to strongly constrain the other parameters of the model.

- The angular distribution of the Z/H in the Higgs–strahlung process is sensitive to the spin–zero of the Higgs particle: at high–energies the Z is longitudinally polarized and the distribution follows the $\sim \sin^2 \theta$ law which unambiguously characterizes the production of a $J^P = 0^+$ particle. The spin–parity quantum numbers of the Higgs bosons can also be checked experimentally by looking at correlations in the production $e^+e^- \rightarrow HZ \rightarrow 4f$ or decay $H \rightarrow WW^* \rightarrow 4f$ processes, as well as in the channel $H \rightarrow \tau^+\tau^-$ for $M_H \lesssim 140$ GeV. An unambiguous test of the CP nature of the Higgs bosons can be made in the process $e^+e^- \rightarrow t\bar{t}H$ or at laser photon colliders in the loop induced process $\gamma\gamma \rightarrow H$.

- The masses of the gauge bosons are generated through the Higgs mechanism and the Higgs couplings to these particles are proportional to their masses. This fundamental prediction has to be verified experimentally. The Higgs couplings to ZZ/WW bosons can be directly determined by measuring the production cross sections in the bremsstrahlung and the fusion processes. In the $e^+e^- \rightarrow H\ell^+\ell^-$ and $H\nu\bar{\nu}$ processes, the total cross section can be measured with a precision less than $\sim 3\%$ at $\sqrt{s} \sim 500$ GeV and with $\int \mathcal{L} = 500$ fb $^{-1}$. This leads to an accuracy of $\lesssim 1.5\%$ on the HVV couplings.

- The measurement of the branching ratios of the Higgs boson are of utmost importance. For Higgs masses below $M_H \lesssim 130$ GeV a large variety of ratios can be measured at the linear collider. The $b\bar{b}, c\bar{c}$ and $\tau^+\tau^-$ branching ratios allow to measure the relative couplings of the Higgs to these fermions and to check the fundamental prediction of the Higgs mechanism that they are proportional to fermion masses. In particular $\text{BR}(H \rightarrow \tau^+\tau^-) \sim m_\tau^2/3\bar{m}_b^2$ allows to make such a test. In addition, these branching ratios, if measured with enough accuracy, could allow to distinguish a Higgs boson in the SM from its possible extensions. The gluonic branching ratio is sensitive to the $t\bar{t}H$ Yukawa coupling [and might therefore give an indirect measurement of this important coupling] and to new strongly interacting particles which couple to the Higgs [such as stop in SUSY extensions of the SM]. The branching ratio into W bosons starts to be significant for Higgs masses of the order of 120 GeV and allows to measure the HWW coupling. The branching ratio of the loop induced $\gamma\gamma$ decay is also very important since it is sensitive to new particles [the measurement of this ratio gives the same information as the measurement of the cross section for Higgs boson production at $\gamma\gamma$ colliders].

- The Higgs coupling to top quarks, which is the largest coupling in the SM, is directly accessible in the process where the Higgs boson is radiated off top quarks, $e^+e^- \rightarrow t\bar{t}H$. For $M_H \lesssim 130$ GeV, the Yukawa coupling can be measured with a precision of less than 5% at $\sqrt{s} \sim 800$ GeV with a luminosity $\int \mathcal{L} \sim 1$ ab $^{-1}$. For $M_H \gtrsim 350$ GeV, the $Ht\bar{t}$ coupling can be derived by measuring the $H \rightarrow t\bar{t}$ branching ratio at higher energies.

- The total width of the Higgs boson, for masses less than ~ 200 GeV, is so small that it cannot be resolved experimentally. However, the measurement of $\text{BR}(H \rightarrow WW)$ allows an indirect determination of Γ_H since the HWW coupling can be determined from the measurement of the Higgs production cross section in the WW fusion process [or from the measurement of the cross section of the Higgs–strahlung process, assuming SU(2) invariance]. The accuracy of the Γ_H measurement follows then from that of the WW branching ratio. [Γ_{tot} can also be measured by using the processes $H \leftrightarrow \gamma\gamma$].

- Finally, the measurement of the trilinear Higgs self–coupling, which is the first non–trivial test of the Higgs potential, is accessible in the double Higgs production processes $e^+e^- \rightarrow ZHH$ [and in the $e^+e^- \rightarrow \nu\bar{\nu}HH$ process at high energies]. Despite its smallness, the cross sections can be determined with an accuracy of the order of 20% at a 500 GeV collider if a high luminosity, $\int \mathcal{L} \sim 1 \text{ ab}^{-1}$, is available. This would allow the measurement of the trilinear Higgs self–coupling with an accuracy of the same order.

An illustration of the experimental accuracies which can be achieved in the determination of the mass, CP–nature, total decay width and the various couplings of the Higgs boson for $M_H = 120$ and 140 GeV is shown in Table 1 for $\sqrt{s} = 350$ GeV (for M_H and the CP nature) and 500 GeV (for Γ_{tot} and all couplings except for g_{Htt}) and $\int \mathcal{L} = 500 \text{ fb}^{-1}$ (except for g_{Htt} where $\sqrt{s} = 1 \text{ TeV}$ and $\int \mathcal{L} = 1 \text{ ab}^{-1}$ are assumed). For the Higgs self–couplings, the error is only on the determination of the cross section, leading to an error slightly larger, $\sim 30\%$, on the coupling. For the test of the CP nature of the Higgs boson, ΔCP represents the relative deviation from the 0^{++} case.

Table 1: Relative accuracies (in %) on Higgs boson mass, width and couplings obtained at TESLA with $\sqrt{s} = 350, 500$ GeV and $\int \mathcal{L} = 500 \text{ fb}^{-1}$ (except for top).

M_H (GeV)	ΔM_H	ΔCP	Γ_{tot}	g_{HWW}	g_{HZZ}	g_{Htt}	g_{Hbb}	g_{Hcc}	$g_{H\tau\tau}$	g_{HHH}
120	± 0.033	± 3.8	± 6.1	± 1.2	± 1.2	± 3.0	± 2.2	± 3.7	± 3.3	± 17
140	± 0.05	–	± 4.5	± 2.0	± 1.3	± 6.1	± 2.2	± 10	± 4.8	± 23

As can be seen, an e^+e^- linear collider with a high–luminosity is a very high precision machine in the context of Higgs physics. This precision would allow the determination of the complete profile of the SM Higgs boson, in particular if its mass is smaller than ~ 140 GeV. It would also allow to distinguish the SM Higgs particle from the lighter MSSM h boson up to very high values of the pseudoscalar Higgs boson mass, $M_A \sim \mathcal{O}(1 \text{ TeV})$. This is exemplified in Fig. 13, where the (g_{Hbb}, g_{HWW}) and $(g_{Hbb}, g_{H\tau\tau})$ contours are shown for a Higgs boson mass $M_H = 120$ GeV produced and measured at a 500 GeV collider with $\int \mathcal{L} = 500 \text{ fb}^{-1}$. These plots are obtained from a global fit which take into account

the experimental correlation between various measurements [37]. In addition to the 1σ and 2σ confidence level contours for the fitted values of the pairs of ratios, the expected value predicted in the MSSM for a given range of M_A is shown.

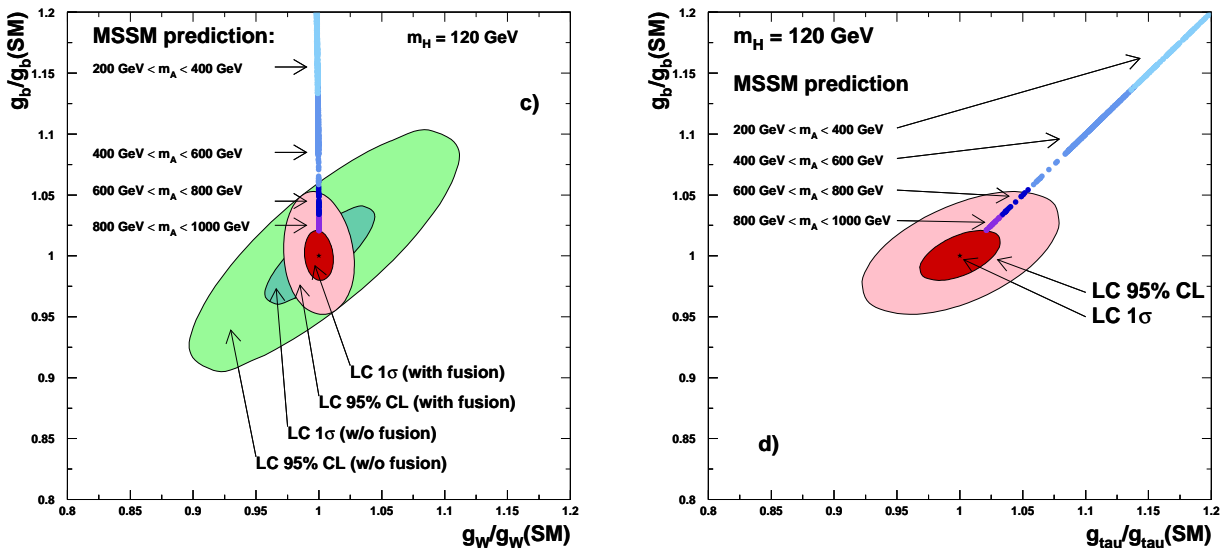


Figure 13: Higgs boson coupling determinations at TESLA for $M_H = 120$ GeV with 500 fb^{-1} of data, and the expected deviations in the MSSM.

5.2 Measurements at the LHC

- At the LHC, the Higgs boson mass can be measured with a very good accuracy. In the range below $M_H \lesssim 400$ GeV, where the total width is not too large, a relative precision of $\Delta M_H/M_H \sim 0.1\%$ can be achieved in the channel $H \rightarrow ZZ^{(*)} \rightarrow 4\ell^\pm$ with 300 fb^{-1} luminosity. In the ‘low mass’ range, a slight improvement can be obtained by considering $H \rightarrow \gamma\gamma$. In the range $M_H \gtrsim 400$ GeV, the precision starts to deteriorate because of the smaller cross sections. However a precision of the order of 1% can still be obtained for $M_H \sim 800$ GeV if theoretical errors, such as width effects, are not taken into account.

- Using the same process, $H \rightarrow ZZ^{(*)} \rightarrow 4\ell^\pm$, the total Higgs width can be measured for masses above $M_H \gtrsim 200$ GeV when it is large enough. While the precision is very poor near this mass value [a factor of two], it improves to reach the level of $\sim 5\%$ around $M_H \sim 400$ GeV. Here, again the theoretical errors are not taken into account.

- The Higgs boson spin can be measured by looking at angular correlations between the fermions in the final states in $H \rightarrow VV \rightarrow 4f$ as in e^+e^- collisions. However the cross sections are rather small and the environment too difficult. Only the measurement of the decay planes of the two Z bosons decaying into four leptons seems promising.

- The direct measurement of the Higgs couplings to gauge bosons and fermions is possible but with a rather poor accuracy. This is due to the limited statistics, the large backgrounds and the theoretical uncertainties from the limited precision on the parton densities and the higher order radiative corrections or scale dependence. An example of determination of cross sections times branching in various channels at the LHC is shown in Fig. 14 from Ref. [14] for a luminosity of 200 fb^{-1} . Solid lines are for gg fusion, dotted lines are for $t\bar{t}H$ associated production with $H \rightarrow b\bar{b}$ and WW and dashed lines are the expectations for the weak boson fusion process. A precision of the order of 10 to 20% can be achieved in some channels, while the vector boson fusion process leads to accuracies of the order of a few percent. However, experimental analyses accounting for the backgrounds and for the detector efficiencies as well as further theory studies for the signal and backgrounds need to be performed to confirm these values. The Higgs boson self-couplings are too difficult to measure at the LHC because of the smallness of the $gg \rightarrow HH$ and $qq \rightarrow HHZ$ cross sections [39] and the large backgrounds.

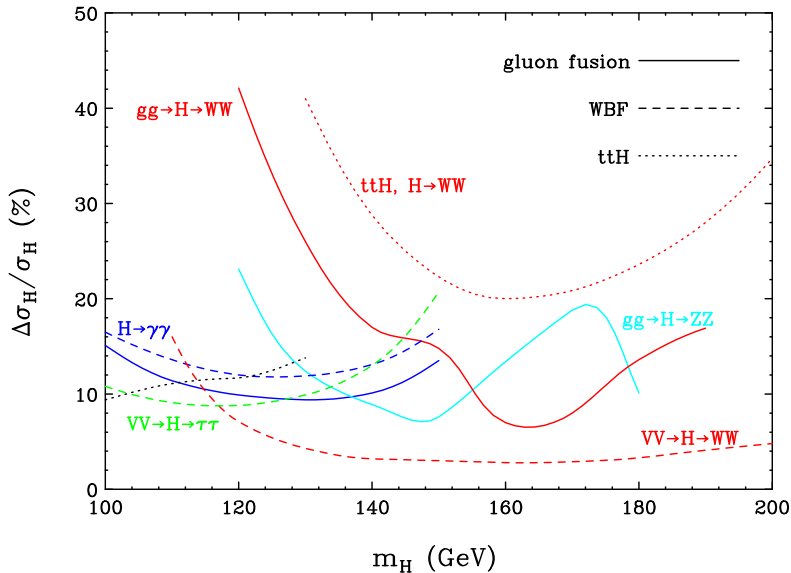


Figure 14: Expected relative errors on the determination of $\sigma \times \text{BR}$ for various Higgs boson search channels at the LHC with 200 fb^{-1} data.

- To reduce the theoretical uncertainties and some experimental errors, it is more interesting to measure ratios of quantities where the overall normalization cancels out. For instance, by using the same production channel and two decay modes, the theory error from higher order corrections and from the poor knowledge of the parton densities drops out in the ratios. A few examples [38] of measurements of ratios of branching ratios or ratios of Higgs couplings squared at the LHC with a luminosity of 300 fb^{-1} are shown in Table 2 [with still some theory errors not included in some cases]. As can be seen, a precision of the order of 10 percent can be reached in these preliminary analyses.

Table 2: Relative accuracies on measurements of ratios of cross sections and/or branching ratios at the LHC with a luminosity of 300 fb^{-1} .

Process	Measurement quantity	Error	Mass range
$\frac{(t\bar{t}H+WH)\rightarrow\gamma\gamma+X}{(t\bar{t}H+WH)\rightarrow b\bar{b}+X}$	$\frac{\text{BR}(H\rightarrow\gamma\gamma)}{\text{BR}(H\rightarrow b\bar{b})}$	$\sim 15\%$	80 – 120 GeV
$\frac{H\rightarrow\gamma\gamma}{H\rightarrow 4\ell^+}$	$\frac{\text{BR}(H\rightarrow\gamma\gamma)}{\text{BR}(H\rightarrow ZZ^*)}$	$\sim 7\%$	120 – 150 GeV
$\frac{t\bar{t}H\rightarrow\gamma\gamma, b\bar{b}}{WH\rightarrow\gamma\gamma, b\bar{b}}$	$\left(\frac{g_{Ht\bar{t}}}{g_{HWW}}\right)^2$	$\sim 15\%$	80 – 120 GeV
$\frac{H\rightarrow ZZ^*\rightarrow 4\ell^+}{H\rightarrow WW^*\rightarrow 2\ell^\pm 2\nu}$	$\left(\frac{g_{HZZ}}{g_{HWW}}\right)^2$	$\sim 10\%$	130 – 190 GeV

A more promising channel would be the vector boson fusion process, $qq \rightarrow WW/ZZ \rightarrow Hqq$ in which $H \rightarrow \tau^+\tau^-$ or WW^* , which would allow the additional measurement of the couplings to τ leptons for instance. A preliminary parton level analysis including this production channel shows that measurements of some Higgs boson couplings can be made at the level of 5–10% statistical error [14]. More work, including full detector simulation, is needed to sharpen these analyses.

6. Conclusions and Complementarity between the LHC and LC

In the SM, global fits of the electroweak data favor a light Higgs boson, $M_H \lesssim 200 \text{ GeV}$, and if the theory is to remain valid up to the GUT scale, the Higgs boson should be lighter than 200 GeV. In supersymmetric extensions of the SM, there is always one light Higgs boson with a mass $M_h \lesssim 130 \text{ GeV}$ in the minimal version and $M_h \lesssim 200 \text{ GeV}$ in more general ones. Thus, a Higgs boson is definitely accessible at next generation experiments.

The detection of such a Higgs particle is possible at the upgraded Tevatron for $M_H \lesssim 130 \text{ GeV}$ and is not a problem at the LHC where even much heavier Higgs bosons can be probed: in the SM up to $M_H \sim 1 \text{ TeV}$ and in the MSSM for M_{A,H,H^\pm} of order a few hundred GeV depending on $\tan\beta$. Relatively light Higgs bosons can also be found at future e^+e^- colliders with c.m. energies $\sqrt{s} \gtrsim 350 \text{ GeV}$; the signals are very clear and the expected high luminosity allows to investigate thoroughly their fundamental properties.

In many aspects, the searches at e^+e^- colliders are complementary to those which will be performed at the LHC. An example can be given in the context of the MSSM. In constrained scenarios, such as the minimal Supergravity model, the heavier H, A and H^\pm bosons tend to have masses of the order of 1 TeV [40] and therefore will escape detection at both the LHC and linear collider. The right-handed panel of Fig. 15 shows the number of Higgs particles in the $(M_A, \tan\beta)$ plane which can be observed at the LHC and in the white area, only the lightest h boson can be observed. In this parameter range, the h

boson couplings to fermions and gauge bosons will be almost SM-like and, because of the relatively poor accuracy of the measurements at the LHC, it would be difficult to resolve between the SM and MSSM (or extended) scenarii. At e^+e^- colliders such as TESLA, the Higgs couplings can be measured with a great accuracy, allowing to distinguish between the SM and the MSSM Higgs boson close to the decoupling limit, i.e. for pseudoscalar boson masses which are not accessible at the LHC. This is exemplified in the right-panel of Fig. 15, where the accuracy in the determination of the Higgs couplings to $t\bar{t}$ and WW are displayed, together with the predicted values in the MSSM for different values of M_A . The two scenarii can be distinguished for pseudoscalar Higgs masses up to 1 TeV.

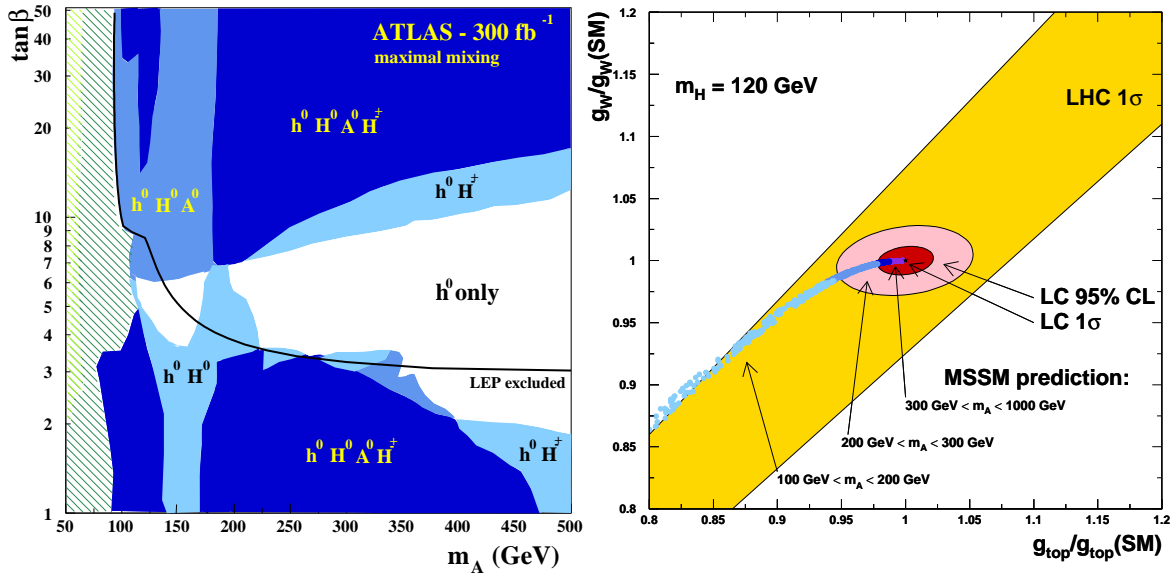


Figure 15: Number of Higgs bosons which can be observed at the LHC in the $(M_A, \tan\beta)$ plane (right) and a comparison of the accuracy in the determination of the $g_{t\bar{t}H}$ and g_{WWH} couplings at the LHC and at TESLA compared to the predictions from MSSM for different values of M_A .

Acknowledgments: I thank the organizers of the WHEPP VII workshop in Allahabad, in particular Biswarup Mukhopadhyaya and Rohini Godbole, for the invitation to the meeting and for the very nice and warm atmosphere. I thank also the people who attended the workshop for very nice (in particular after dinner) physics and non-physics discussions. Special thanks go to the “guru” K. Sridhar for taking care of our souls and our stomachs.

References

- [1] P.W. Higgs, *Phys. Rev. Lett.* 12 (1964) 132; F. Englert and R. Brout, *Phys. Rev. Lett.* 13 (1964) 321; G.S. Guralnik, C.R. Hagen and T.W. Kibble, *Phys. Rev. Lett.* 13 (1964) 585.
- [2] For a review on the Higgs sector in the SM and MSSM see: J.F. Gunion, H.E. Haber, G.L. Kane and S. Dawson, “The Higgs Hunter’s Guide”, Addison–Wesley, Reading 1990.
- [3] The LEP Higgs working group, hep-ex/0107029 and hep-ex/0107030.
- [4] The LEP and SLC Electroweak Working Groups, hep-ex/0112021.
- [5] B.W. Lee, C. Quigg and H.B. Thacker, *Phys. Rev.* 16 (1977) 1519.
- [6] See e.g.: T. Hambye and K. Riesselman, *Phys. Rev.* D55 (1997) 7255.
- [7] For recent reviews, see: M. Drees and S. Martin, hep-ph/9504324; S. Martin, hep-ph/9709356; J. Bagger, hep-ph/9604232; The GDR–SUSY MSSM Working Group, hep-ph/9901246.
- [8] M. Carena et al., *Nucl. Phys.* B580 (2000) 29; J.R. Espinosa and R.J. Zhang, *Nucl. Phys.* B586 (2000)3; G. Degrassi, P. Slavich and F. Zwirner, *Nucl. Phys.* B611 (2001) 403 and hep-ph/0112177.
- [9] M. Drees, *Int. J. Mod. Phys.* A4 (1989) 87; S.F. King and P.L. White, *Phys. Rev.* D52 (1995) 4183; U. Ellwanger, M. Rausch de Traubenberg and C. A. Savoy, *Nucl. Phys.* B492 (1997) 21.
- [10] J.R. Espinosa and M. Quiros, *Phys. Rev. Lett.* 81 (1998) 516.
- [11] E. Boos, A. Djouadi, M. Muhlleitner and A. Vologdin, hep-ph/0205160.
- [12] M. Carena et al., Report of the Higgs WG for “RUN II at the Tevatron”, hep-ph/0010338.
- [13] CMS Coll., Technical Proposal, report CERN/LHCC/94-38 (1994); ATLAS Coll., Technical Design Report, CERN/LHCC/99-15 (1999); Proceedings of the Les Houches Workshops: A. Djouadi et al., hep-ph/0002258 (1999) and D. Cavalli et al., hep-ph/0203056 (2001).
- [14] D. Zeppenfeld, R. Kinnunen, A. Nikitenko and E. Richter-Was, *Phys. Rev.* D62 (2000) 013009.

- [15] E. Accomando, Phys. Rept. 299 (1998) 1; American Linear Collider Working Group (T. Abe et al.), hep-ex/0106057; J. Bagger et al., hep-ex/0007022; H. Murayama and M. Peskin, Ann. Rev. Nucl. Part. Sci. 46 (1996) 533; A. Djouadi, Int. J. Mod. Phys. A10 (1995) 1.
- [16] TESLA Technical Design Report, Part III, DESY-01-011C, hep-ph/0106315.
- [17] A. Djouadi, J. Kalinowski and M. Spira, Comput. Phys. Commun. 108 (1998) 56; A. Djouadi, M. Spira and P. M. Zerwas, Z. Phys. C70 (1996) 427; S. Moretti and W.J. Stirling, Phys. Lett. B347 (1995) 291; A. Djouadi, J. Kalinowski and P. M. Zerwas, Z. Phys. C70 (1996) 435; A. Djouadi and P. Gambino, Phys. Rev. D51 (1995) 218.
- [18] H. Baer et al., Phys. Rev. D36 (1987) 1363; K. Griest, H.E. Haber, Phys. Rev. D37 (1988) 719; J.F. Gunion and H.E. Haber, Nucl. Phys. B307 (1988) 445; A. Djouadi et al., Phys. Lett. B376 (1996) 220 and Z. Phys. C 74 (1997) 93; A. Bartl et al., Phys. Lett. B389 (1996) 538; A. Djouadi, Mod. Phys. Lett. A14 (1999) 359.
- [19] H. Georgi et al., Phys. Rev. Lett. 40 (1978) 692; S.L. Glashow, D.V. Nanopoulos and A. Yildiz, Phys. Rev. D18 (1978) 1724; R.N. Cahn and S. Dawson, Phys. Lett. B136 (1984) 196; K. Hikasa, Phys. Lett. B164 (1985) 341; G. Altarelli, B. Mele and F. Pitolli, Nucl. Phys. B287 (1987) 205; Z. Kunszt, Nucl. Phys. B247 (1984) 339; J. Gunion, Phys. Lett. B253 (1991) 269.
- [20] M. Spira, Fortschr. Phys. 46 (1998) 203; see also: hep-ph/9711394 and hep-ph/9810289.
- [21] A. Djouadi, M. Spira and P.M. Zerwas, Phys. Lett. B264 (1991) 440; S. Dawson, Nucl. Phys. B359 (1991) 283; M. Spira et al., Phys. Lett. B318 (1993) 347 and Nucl. Phys. B453 (1995) 17; S. Dawson, A. Djouadi and M. Spira, Phys. Rev. Lett. 77 (1996) 16; S. Catani et al., JHEP 0105 (2001) 025; R.V. Harlander and W. Kilgore, hep-ph/0201206.
- [22] T. Han, G. Valencia and S. Willenbrock, Phys. Rev. Lett. 69 (1992) 3274; D.A. Dicus and S. Willenbrock, Phys. Rev. D39 (1989) 751; A. Djouadi and M. Spira, Phys. Rev. D62 (2000) 014004; W. Beenakker et al., Phys. Rev. Lett. 87 (2001) 201805; L. Reina and S. Dawson, Phys. Rev. Lett. 87 (2001) 201804.
- [23] A. Bawa, C. Kim and A. Martin, Z. Phys. C47 (1990) 75; V. Barger, R. Phillips and D.P. Roy, Phys. Lett. B324 (1994) 236; S. Moretti and K. Odagiri, Phys. Rev. D55 (1997) 5627; J. Gunion, Phys. Lett. B322 (1994) 125; F. Borzumati, J.L. Kneur and N. Polonsky, Phys. Rev. D60 (1999) 115011; D. Miller, S. Moretti, D.P. Roy and W. Stirling, Phys. Rev. D61 (2000) 055011.

- [24] M. Bisset, M. Guchait and S. Moretti, hep-ph/0010253; F. Moortgat, hep-ph/0105081.
- [25] A. Djouadi, Phys. Lett. B435 (1998) 101.
- [26] A. Djouadi, J.L. Kneur, G. Moultaka, Phys.Rev.Lett. 80 (1998) 1830 and Nucl.Phys. B569 (2000) 53; G. Bélanger, F. Boudjema, T. Kon, V. Lafage, Eur.Phys.J. C9 (1999) 511; A. Dedes and S. Moretti, Eur.Phys.J. C10 (1999) 515 and Phys. Rev. D60 (1999) 015007.
- [27] A. Bartl, W. Majerotto and N. Oshimo, Phys.Lett.B216 (1989) 233; H. Baer et al., Phys. Rev. D46 (1992) 303; A. Datta et al., Phys. Rev. D65 (2002) 015007; F. Moortgat, hep-ph/0112046.
- [28] U. Ellwanger, J.F. Gunion and C. Hugonie, hep-ph/0111179.
- [29] J. Ellis, M.K. Gaillard and D.V. Nanopoulos, Nucl. Phys. B106 (1976) 292; B.W. Lee, C. Quigg and H.H. Thacker, Phys. Rev. D16 (1977) 1519; J.D. Bjorken, SLAC Report 198 (1976); B. Ioffe and V.A. Khoze, Sov. J. Part. Nucl. 9, (1978) 50; D.R.T. Jones and S.T. Petcov, Phys. Lett. B84 (1979) 440; R.N. Cahn and S. Dawson, Phys. Lett. B136 (1984) 196; G. Altarelli, B. Mele and F. Pitolli, Nucl. Phys. B287 (1987) 205; V. Barger et al., Phys. Rev. D49 (1994) 79; W. Kilian, M. Krämer and P.M. Zerwas, Phys. Lett. B373 (1996) 135; A. Djouadi, J. Kalinowski and P. M. Zerwas, Mod. Phys. Lett. A7 (1992) 1765 and Z. Phys. C54 (1992) 255.
- [30] A. Djouadi, H.E. Haber and P.M. Zerwas, Phys. Lett. B375 (1996) 203; A. Djouadi, W. Kilian, M.M. Muhlleitner and P.M. Zerwas, Eur. Phys. J.C10 (1999) 27; P. Osland, P.N. Pandita, Phys. Rev. D59 (1999) 055013; F. Boudjema and A. Semenov, hep-ph/0201219.
- [31] J. Ellis et al., Phys. Rev. D39 (1989) 844; A. Djouadi et al., Z. Phys. C57 (1993) 569 and Z. Phys. C74 (1997) 93; P.M. Zerwas (ed.) et al., hep-ph/9605437;
- [32] M. Berggren, R. Keranen and A. Sopczak, Eur. Phys. J. direct C8 (2000) 1; J.F. Gunion et al., hep-ph/0112334; A. Djouadi, P.M. Zerwas and J. Zunft, Phys. Lett. B259 (1991) 175.
- [33] J. R. Espinosa and J. F. Gunion, Phys. Rev. Lett. 82 (1999) 1084.
- [34] ECFA/DESY Photon Collider Working Group, DESY-2001-011, hep-ex/0108012.

- [35] J.F. Gunion and H. Haber, Phys. Rev. D48 (1993) 5109; D. Borden, D. Bauer and D. Caldwell, Phys. Rev. D48 (1993) 4018; M. Baillargeon, G. Belanger and F. Boudjema, Phys. Rev. D51 (1995) 4712; J.I. Illana et al., Eur. Phys. J.C1 (1998) 149; I. Ginzburg and I. Ivanov, Phys. Lett. B408 (1997) 325; E. Boos et al., Phys. Lett. B427 (1998) 189.
- [36] J.I. Illana, hep-ph/9912467; M.M. Muhlleitner, M. Kramer, M. Spira and P.M. Zerwas, Phys. Lett. B508 (2001) 311; D. Asner, J. Gronberg and J. Gunion, hep-ph/0110320.
- [37] Marco Battaglia and Klaus Desch, hep-ph/0101165.
- [38] F. Gianotti, talk given at the LHC Committee, CERN, 5/7/2000.
- [39] E. Glover and J. van der Bij, Nucl. Phys. B309 (1988) 282; T. Plehn, M. Spira and P. Zerwas, Nucl. Phys. B479 (1996) 46; R. Lafaye, D. Miller, M. Muhlleitner and S. Moretti, hep-ph/0002238. A. Djouadi, W. Kilian, M. Muhlleitner and P. Zerwas, Eur. Phys. J. C10 (1999) 45.
- [40] For recent analyses, see: M. Battaglia et al., Eur. Phys. J. C22 (2001) 535; A. Djouadi, M. Drees and J.L. Kneur, JHEP 0108 (2001) 055; L. Roszkowski, R. Ruiz de Austri and T. Nihei, JHEP 0108 (2001) 024; A.B. Lahanas and V.C. Spanos, Eur. Phys. J. C23 (2002) 185; V. Barger and C. Kao Phys. Lett. B518 (2001) 117; B.C. Allanach et al., hep-ph/0202233.